0026-895X/07/7203-502–513$20.00
MOLECULAR PHARMACOLOGY
Copyright © 2007 The American Society for Pharmacology and Experimental Therapeutics
Mol Pharmacol 72:502–513, 2007

Vol. 72, No. 3
37085/3240825
Printed in U.S.A.

Localization of the Mouse 5-Hydroxytryptamine$_{1A}$ Receptor in Lipid Microdomains Depends on Its Palmitoylation and Is Involved in Receptor-Mediated Signaling

Ute Renner, Konstantin Glebov, Thorsten Lang, Ekaterina Papusheva, Saju Balakrishnan, Bernhard Keller, Diethelm W. Richter, Reinhard Jahn, and Evgeni Ponimaskin

Abteilung Neuro- und Sinnesphysiologie, Physiologisches Institut, Universität Göttingen, Göttingen, Germany (U.R., K.G., E.P., S.B., B.K., D.W.R., E.P.); Center of Molecular Physiology of the Brain, Göttingen, Germany (U.R., D.W.R., E.P.); and Department of Neurobiology, Max-Planck-Institute for Biophysical Chemistry, Göttingen, Germany (T.L., R.J.)

Received April 13, 2007; accepted May 31, 2007

ABSTRACT

In the present study, we have used wild-type and palmitoylation-deficient mouse 5-hydroxytryptamine$_{1A}$ receptor (5-HT1A) receptors fused to the yellow fluorescent protein- and the cyan fluorescent protein (CFP)-tagged α_{i3} subunit of heterotrimeric G-protein to study spatiotemporal distribution of the 5-HT1A-mediated signaling in living cells. We also addressed the question on the molecular mechanisms by which receptor palmitoylation may regulate communication between receptors and G_i-proteins. Our data demonstrate that activation of the 5-HT1A receptor caused a partial release of $G\alpha_i$ protein into the cytoplasm and that this translocation is accompanied by a significant increase of the intracellular Ca^{2+} concentration. In contrast, acylation-deficient 5-HT1A mutants failed to reproduce both $G\alpha_{i3}$-CFP relocation and changes in $[Ca^{2+}]_i$ upon agonist stimulation. By using gradient centrifugation and copatching assays, we also demonstrate that a significant fraction of the 5-HT1A receptor resides in membrane rafts, whereas the yield of the palmitoylation-deficient receptor in these membrane microdomains is reduced considerably. Our results suggest that receptor palmitoylation serves as a targeting signal responsible for the retention of the 5-HT1A receptor in membrane rafts. More importantly, the raft localization of the 5-HT1A receptor seems to be involved in receptor-mediated signaling.

G-protein-coupled receptors (GPCRs) play a central role in transducing extracellular signals across the cell membrane with high sensitivity and specificity. These integral membrane proteins represent the largest and most versatile group of receptors with an essential role in the regulation of almost all physiological processes in both mammalian and nonmammalian species (Pierce et al., 2002). A large body of evidence obtained in different experimental systems suggests that the specificity of GPCR-mediated signaling is partially achieved by the selective compartmentalization of signaling components within specific microdomains on the plasma membrane (Anderson, 1998; Chini and Parenti, 2004). These microdomains, named lipid rafts and caveolae, represent the membrane subdomains differing from the bulk membrane by enrichment in specific proteins and lipids. They are characterized by a high content of glycosphingolipid and cholesterol in the outer leaflet of the lipid bilayer that gives them a gel-like liquid-ordered (l_o) structure (Brown and London, 1998). In contrast to the membranes in the conventional disordered phase, lipid rafts and caveolae are resistant to the low-temperature solubilization by nonionic detergents (Brown and London, 1998) allowing for their biochemical separation as a result of the differential flotation in the density gradients.

Lipid rafts and caveolae have been shown to be involved in

These studies were supported by the fund of the Medical School at the University of Göttingen and by the Deutsche Forschungsgemeinschaft through the Center of Molecular Physiology of the Brain (to E.G.P.) and grant PO 732.
U.R. and K.G. contributed equally to this work.
Article, publication date, and citation information can be found at http://molpharm.aspetjournals.org.
doi:10.1124/mol.107.037085.

ABBREVIATIONS: GPCR, G-protein-coupled receptor; 5-HT1A, mouse 5-hydroxytryptamine$_{1A}$ receptor; CTX, cholera toxin; CFP, cyan fluorescent protein; DRM, detergent-resistant membrane fraction; MβCD, methyl-β-cyclodextrin; PTx, pertussis toxin; YFP, yellow fluorescent protein; l_o, liquid-ordered; HA, hemagglutinin; WT, wild-type; PBS, phosphate-buffered saline; DTT, dithiothreitol; PAGE, polyacrylamide gel electrophoresis; GFP, green fluorescent protein; Erk, extracellular signal-regulated kinase; AM, acetoxymethyl ester; CHO, Chinese hamster ovary; Mut, acylation-deficient; GTPγS, guanosine 5′-3-*O*-(thio)triphosphate; 8-OH-DPAT, 8-hydroxy-2-dipropylaminotetralin; KGlu buffer, potassium glutamate, potassium acetate, and HEPES; TMA-DPH, 1-(4-trimethylammoniumphenyl)-6-phenyl- 1,3,5-hexatriene-*p*-toluenesulfonate; WAY100635, [*O*-methyl-3*H*]-*N*-(2-(4-(2-methoxyphenyl)-1-piperazinyl)ethyl)-*N*-(2-pyridinyl)cyclohexanecarboxamide trihydrochloride.

the regulation of various cell functions, including the intracellular sorting of proteins and lipids (Sprong et al., 2001), the establishment of cell polarity (Mañes et al., 2003), and the fine tuning of signaling processes (Simons and Toomre, 2000). The detection of numerous signaling proteins within the detergent-resistant membrane fractions (DRMs) led to the assumption that lipid rafts represent scaffold platforms, which facilitate signal transduction by spatially recruiting signaling components and by preventing an inappropriate cross-talk between pathways (Okamoto et al., 1998; Foster et al., 2003). Little is known about the molecular determinants regulating localization of signaling proteins and particularly GPCRs in lipid microdomains. Several possible mechanisms for rafts targeting have been proposed, including 1) specific interaction with the lipid components of rafts/caveolae such as cholesterol (Eroglu et al., 2003; Pucadyil and Chattopadhyay, 2004); 2) direct interaction with the scaffolding domain of caveolin (Okamoto et al., 1998); and 3) the covalent attachment of saturated fatty acyl chains, including myristic and palmitic acids (Moffett et al., 2000; Zacharias et al., 2002).

In the present study, we have used wild-type and palmitoylation-deficient 5-HT1A receptors tagged to the yellow fluorescent protein (YFP)- and the cyan fluorescent protein (CFP)-tagged α_i-subunit of heterotrimeric G-protein (Leaney et al., 2002) to study spatiotemporal distribution of the 5-HT1A-mediated signaling. In addition, we analyzed whether receptor palmitoylation is involved in targeting the receptor to the membrane subdomains.

The 5-HT1A receptor belongs to the GPCR superfamily and is the most extensively characterized member of the serotonin (5-hydroxytryptamine or 5-HT) receptor family. This receptor was found to be involved in a number of physiological and behavioral effects, such as regulation of mood (Sibille and Hen, 2001), neuroendocrine responses (Burnet et al., 1996), body temperature (Overstreet, 2002), neurogenesis (Radley and Jacobs, 2002), and respiratory activity (Richter et al., 2003). The 5-HT1A receptor has also been shown to play an important role in several psychiatric disorders, and its partial agonists are widely used in the treatment of depression and anxiety syndromes (Gordon and Hen, 2004).

The 5-HT1A receptor is coupled to a variety of effectors via pertussis toxin-sensitive G-proteins of the $G_{i/o}$ family (De Vivo and Maayani, 1986; Dumuis et al., 1988). Receptor-induced activation of $G\alpha_i$ subunits results in the inhibition of adenylyl cyclase and a subsequent decrease of cAMP levels in both homologous and heterologous systems (De Vivo and Maayani, 1986; Nebigil et al., 1995). Besides effects mediated by $G\alpha_{i/o}$ subunits, activation of the 5-HT1A receptor also leads to the $G\beta\gamma$-mediated activation of K^+ currents, stimulation of phospholipase C, and activation of mitogen-activated protein kinase extracellular signal-regulated kinase 2 (Erk2) (Andrade et al., 1986; Fargin et al., 1991; Garnovskaya et al., 1996).

We have shown recently that the recombinant 5-HT1A receptor is modified by covalently attached palmitate and that palmitoylation of the 5-HT1A receptor is irreversible and insensitive to agonist stimulation (Papoucheva et al., 2004). Two conserved cysteine residues 417 and 420 located in the C-terminal domain were identified as acylation sites of the 5-HT1A receptor. When palmitoylated cysteines were mutated, communication between receptors and $G\alpha_i$ subunits was completely abolished, indicating that palmitoylation of the 5-HT1A receptor is critical for G_i-protein coupling/effector signaling (Papoucheva et al., 2004).

Materials and Methods

Recombinant DNA Procedures. All basic DNA procedures were performed as described by Sambrook et al. (1989). The $G\alpha_{i3}$-CFP cDNA was kindly provided by Dr. Andrew Tinker (University College, London, UK). The construction of the HA-tagged 5-HT1A and generation of the palmitoylation-deficient 5-HT1A mutant (C417S, C420S) have been described previously (Papoucheva et al., 2004). To prepare a 5-HT1A-YFP fusion construct, cDNA encoding for the 5-HT1A receptor was amplified by polymerase chain reaction with the specific primer Chimera sense-KpnI (5′-ATTCCGGTACCGCGAGGGAGATCCCCTTG-3′) and either with Chimera antisense wild-type (WT)-KpnI (5′-ATCATGGTACCGGGCGGCAGAACTTGCAC-3′) for wild-type or Chimera antisense DM-KpnI (5′-ATCATGGTACCGGG-CGGGAGAACTTGGAC-3′) for acylation-deficient mutant. The amplified fragments were cloned into the KpnI site of the pEYFP-N1 vector (Clontech, Mountain View, CA), so that the YFP coding sequence was located in-frame at the C-terminal end of the 5-HT1A receptor. All constructs were verified by DNA sequencing of the final plasmids.

Adherent Cell Culture and Transfection. NIH-3T3 and neuroblastoma N1E-115 cells were grown in Dulbecco's modified Eagle's medium containing 10% fetal calf serum and 1% penicillin/streptomycin at 37°C under 5% CO_2. For transient transfection, cells were seeded at low density (8×10^5) in 35-mm dishes or in 10-mm coverslips (5×10^5) and transfected with appropriate vectors using Lipofectamine2000 Reagent (Invitrogen, Carlsbad, CA) according to the manufacturer's instruction. Six hours after transfection, cells were serum-starved for different time intervals before analysis. To prepare the cell line stably expressing the YFP-tagged receptor, the NIH-3T3 cells were seeded into 35-mm dishes and transfected either with the wild-type or acylation-deficient 5-HT1A-YFP constructs. After 2 weeks' incubation in the selective medium containing G-418 (Geneticin, 1 mg/ml; Invitrogen), single colonies were collected and plated onto separate 60-mm dishes. The stably transfected cell lines were tested for the expression level of the recombinant protein by immunoblotting and radioligand binding assay.

Biotinylation and Isolation of Cell Surface Proteins. For biotinylation assay, transiently transfected N1E-115 cells (5×10^6) expressing HA- or YFP-tagged 5-HT1A receptors were treated according to the manufacturer's protocol (Pierce, Rockford, IL). In brief, cells were washed three times with ice-cold PBS and incubated for 30 min at 4°C in PBS (100 mM Na_2HPO_4 and 150 mM NaCl, pH 7.2) containing 0.25 mg/ml sulfosuccinimidyl 2-(biotinamido)-ethyl-1,3-dithiopropionate. Cells were harvested, centrifuged at 500*g* for 5 min, and washed with ice-cold Tris-buffered saline (25 mM Tris and 150 mM NaCl, pH 7.2). The cells were lysed, and lysates were cleared by centrifugation at 10,000*g* for 2 min. The biotinylated proteins were isolated from the supernatant with immobilized NeutrAvidin during 1-h incubation at room temperature. Biotinylated proteins were eluted with 50 μl of SDS sample buffer containing 50 mM DTT. Biotinylated and unbound proteins were separated by 12% SDS-PAGE followed by immunoblotting with anti-HA (Santa Cruz Biotechnology, Santa Cruz, CA) or anti-GFP (Abcam, Cambridge, MA) antibodies.

Assay for [Eu]GTPγS Binding. Agonist-promoted binding of [Eu]GTPγS to $G\alpha_i$ protein was performed according to the method described by Barr et al. (1997). In brief, 10 μg of membranes from transfected N1E-115 cells were resuspended in 55 μl of 50 mM Tris-HCl buffer (2 mM EDTA, 100 mM NaCl, 3 mM $MgCl_2$, and 1 μM GDP, pH 7.4) and incubated without or with different concentrations of 8-OH-DPAT at room temperature for 10 min. In several experiments, WAY100635 at 1 μM concentration was added to the mem-

branes 5 min before agonist. After adding [Eu]GTPγS (PerkinElmer Life and Analytical Sciences, Boston, MA) to a final concentration of 10 nM, samples were incubated for 1.5 h at room temperature. The reaction was terminated by adding 600 μl of 50 mM Tris-HCl, pH 7.5, containing 20 mM $MgCl_2$, 150 mM NaCl, 0.5% Nonidet P-40, 200 μg/ml aprotinin, 100 μM GDP, and 100 μM GTP and incubated for 15 min on the ice. The samples were then incubated for 1.5 h with 10 μl of antibody raised against $G\alpha_{i3}$ protein (Santa Cruz) followed by 1.5-h incubation with 30 μl of Sepharose-Protein G beads (Sigma, St. Louis, MO). Immunoprecipitates were washed, heated at 37°C for 15 min in 0.2 ml of 0.5% SDS, centrifuged, and supernatants were subjected to the fluorescence detection. Fluorescence of europium was measured using fluorescent plate reader MithrasLB680 (Berthold Technologies, Bad Wildbad, Germany) at excitation of 315 nm and emission of 615 nm. The data were fitted to a sigmoidal function and analyzed using Matlab software (The MathWorks, Natick, MA).

Erk1/2 Phosphorylation Assay. Serum-starved, transiently or stably transfected NIH-3T3 cells (7×10^5) were stimulated for 5 min with 10 μM 8-OH-DPAT, washed with PBS, and lysed in loading buffer. Equal amounts of proteins in lysates were separated by SDS-PAGE and then subjected to immunoblot. The membranes were probed either with antibodies raised against phosphorylated Erk1/2 (phospho-p42/44; 1:2000 dilution) or against total Erk (p42/44; 1:1000 dilution). To compare the level of receptor expression, membranes were probed with antibodies raised against GFP (1:500; Abcam). Amounts of the phosphorylated and total Erk1/2 were quantified by densitometric measurements using GelPro Analyzer version 3.1 software (Leeds Instruments, Irving, TX).

Radioligand Binding Assay. Membrane preparation of transiently or stably transfected cells was performed according to the protocol described by Claeysen and coworkers (1999). For saturation binding assay, indicated concentrations of [^{3}H]8-OH-DPAT (GE Healthcare, Chalfont St. Giles, Buckinghamshire, UK) were added to 10 μg of the membrane fraction diluted in assay buffer (20 mM HEPES, pH 7.4, 1 mM EDTA, 1 mM EGTA, 6 mM $MgCl_2$, and 0.1% bovine serum albumin). The final volume was 200 μl, and nonspecific binding was determined by the addition of 10 μM concentration of unlabeled 5-HT. After 2.5-h incubation at 20°C, the reaction was terminated by rapid filtration of the samples through GF/B filters (Whatman, Clifton, NJ) presoaked in 1% polyethylenimine using a Brandel cell harvester (Brandel, Gaithersburg, MD). The membranes were washed four times with ice-cold PBS, and the radioactivity was measured by scintillation counting. Data were fitted with the one-site saturation binding model by pharmacology module of SigmaPlot 8.02 software (SPSS Inc., Chicago, IL).

Ca^{2+} Imaging. For intracellular calcium measurements, 5 μM Fura-2/AM (Invitrogen) was added to serum-free culture medium containing 100 ng/ml pertussis toxin, and cells were incubated for 60 min at 37°C under 5% CO_2. Fluorescence measurements of the cells were done in artificial cerebrospinal fluid (118 mM NaCl, 3 mM KCl, 1 mM $MgCl_2$, 25 mM $NaHCO_3$, 1 mM NaH_2PO_4, 1.5 mM $CaCl_2$, and 30 mM glucose, pH 7.4) bubbled with carbogen. Receptors were stimulated by adding 8-OH-DPAT (30 μM) to the bath solution. Fura-2/AM was alternately excited, and 356- and 385-nm emitted light was directed to a dichroic mirror with mid-reflection at 425 nm, filtered by a band-pass filter (505–530 nm) and collected using a charge-coupled device camera (Sensicam; Optikon, Kitchener, ON, Canada). Fluorescence values were calculated as the ratio of fluorescence intensities F/F_0.

Cell Fractionation and Immunoblotting. Transiently transfected neuroblastoma N1E-115 cells expressing 5-HT1A-YFP and $G\alpha_{i3}$-CFP constructs were incubated with 100 ng/ml pertussis toxin (Sigma) during the serum starvation. After stimulation with 30 μM 8-OH-DPAT for 30 s, cells were immediately harvested in ice-cold extraction buffer (10 mM Tris/HCl, pH 7.4, 1 mM EDTA, 150 mM NaCl, 1 mM DTT, 20 μM leupeptin, and 2 μg/ml aprotinin) and homogenized. After centrifugation at 8500 rpm for 5 min, supernatant was centrifuged at 60,000 rpm at 4°C for 30 min on the Beckman Coulter ultracentrifuge with TLA120.2 rotor to separate membrane and cytosolic fraction (Beckman Coulter, Fullerton, CA). The pellets and the supernatants (the latter after extraction with 10% trichloroacetic acid) were separated by 10% SDS-PAGE. Proteins were transferred to Hybond nitrocellulose membrane (Amersham) and probed either with antibodies raised against $G\alpha_{i3}$ (Santa Cruz; 1:1000 diluted in PBS/Tween 20) or against GFP (Abcam; diluted 1:5000 in PBS/Tween 20). Proteins were detected using the enhanced chemiluminescence detection reagents (GE Healthcare).

Time-Lapse Confocal Microscopy. Neuroblastoma N1E-115 cells were cotransfected with $G\alpha_{i3}$-CFP and 5-HT1A-YFP constructs at the DNA ratio 2:1 or 4:1, incubated with 100 ng/ml pertussis toxin (Sigma) during the serum starvation, and then monitored under an inverted confocal laser-scan microscope LSM510-Meta (Carl Zeiss, Jena, Germany) with a 63 × 1.2 numerical aperture water-immersion objective using 458 nm line of an argon laser. Experiments were performed at 37°C in Tyrode's buffer (150 mM NaCl, 10 mM HEPES, 10 mM glucose, 5 mM KCl, 2 mM $CaCl_2$, 1 mM $MgCl_2$, and 100 ng/ml PTx, pH 7.4). For receptor stimulation, 8-OH-DPAT at final concentration of 30 μM was added to the bath. For detection of individual fluorophores, spectral range for λ stack acquisition was set from 462 to 580 nm, yielding a 12-image stack with 10.7-nm increments. The reference spectra of CFP- and YFP-chimera were recorded for each experiment from the cells expressing the individual construct, and the spectral separation was achieved by the linear unmixing function of the LSM Meta software. In the time-lapse analysis, 1-μm optical *z*-sections were captured at each time point before and during treatment with 8-OH-DPAT. The time interval between successive scans was 10 s. For quantitative analysis of $G\alpha_{i3}$-CFP distribution, *z*-sections were projected onto one plane, and the region of interest corresponding to the maximal cytoplasm area was selected for each cell. Changes in CFP-fluorescence intensity were determined from the equation $(F_{post} - F_{pre}) \times 200/F_{pre}$, where F_{pre} and F_{post} are the mean of fluorescence intensity before and during agonist treatment, respectively. Multiplication by 200 was used to span the grayscale spectrum of 8-bit images. Before calculations, images were smoothened using a low-pass Gaussian filter of a 7 × 7-pixel kernel. Statistical evaluation was performed using the paired *t* test applied to compare the averaged values derived from at least three independent experiments.

Gradient Centrifugation. Separation of detergent-resistant membranes derived from the stably transfected NIH-3T3 cells (1×10^6) and transiently transfected CHO cells (1×10^6) growing on 35-mm dishes was performed as described by Harder and coworkers (1998). For cholesterol depletion, cells were washed twice with culture medium without fetal calf serum and antibiotic and treated with 15 mM methyl-β-cyclodextrin for 45 min on ice. Cells were lysed in buffer containing 25 mM Tris/HCl, pH 7.4, 150 mM NaCl, 5 mM EDTA, 1 mM DTT, 10% sucrose, 1% Triton X-100, 1 mM phenylmethylsulfonyl fluoride, 10 μM leupeptin, and 2 μg/ml aprotinin, and lysates (1.2 mg of protein/ml) were mixed with the double volume of 60% Optiprep gradient medium (Nycomed Pharma, Zurich, Switzerland). The resulting 40% Optiprep mixture was transferred into the ultracentrifuge tube and overlaid with steps of each 35, 30, 25, 20, and 0% Optiprep in buffer containing 25 mM Tris/HCl, pH 7.4, 150 mM NaCl, 5 mM EDTA, 1 mM DTT, 10% sucrose, 1% Triton X-100, 1 mM phenylmethylsulfonyl fluoride, 10 μM leupeptin, and 2 μg/ml aprotinin. The gradients were centrifuged for 5 h at 50,000 rpm in the TLS-55 rotor of the ultracentrifuge TL-100 (Beckman). Six fractions were collected from the top of the gradient and trichloroacetic acid-precipitated. The pellets were analyzed by SDS-PAGE followed by immunoblot analysis with appropriate antibodies.

Copatching Assay and Line-Scan Analysis. For preparation of membrane sheets, stably transfected NIH-3T3 cells were treated according to the procedure described by Avery and coworkers (2000). Copatching of YFP-fused receptors and GM1 was carried out by simultaneous incubation of unfixed membrane sheets with goat anti-

GFP antibody (Abcam; 1:1000 dilution) and cholera-toxin (Sigma, 1 μg/ml). Incubation was performed in KGlu buffer (120 mM potassium glutamate, 20 mM potassium acetate, and 20 mM HEPES, pH 7.2) containing 0.5% bovine serum albumin for 60 min at 37°C. Membranes were washed and fixed in 4% phosphonoformic acid for 60 min. The fixed sheets were incubated with mouse anti-cholera toxin (CTX) antibodies with 1:1000 dilution followed by incubation with Alexa Fluor 546-conjugated rabbit anti-mouse antibody (1:500). Before imaging, membranes were stained with TMA-DPH which was directly added to the bath solution. For cholesterol depletion, membrane sheets were treated for 10 min with 5 mM methyl-β-cyclodextrin (Sigma) in KGlu buffer before copatching. For the line-scan analysis, membrane sheets were imaged using Zeiss Axiovert 100 TV fluorescence microscope with a 100 × 1.4 numerical aperture Plan-Achromate objective and a back-illuminated frame transfer charge-coupled device camera. Membrane sheets were imaged in three channels, blue for TMA-DPH (430 nm), green for 5-HT1A-YFP (515 nm), and red for Alexa546-CTX (546 nm). Red and green channels were aligned by color align function of MetaMorph software (Molecular Devices, Sunnyvale, CA) using fluorescent beads (TetraSpec microspheres 0.2 μm; Molecular Probes), which were added to every membrane preparation.

For colocalization analysis, 20 lines (25 pixels/line) per image were drawn across clustered receptors, whereas red channel was switched off. Distance between maximal intensities of red and green pixels in each line was determined on the merge pictures using line scan function of the MetaMorph software, and when the distance was less than two pixels, a colocalization event was counted. For normalization, the counting protocol was repeated after horizontal flipping of the red channel.

Results

Generation and Functional Properties of 5-HT1A-YFP Fusion Constructs. To study 5-HT1A receptor-mediated signaling processes in living cells, enhanced YFP was fused to the C-terminal domain of the wild-type (WT-YFP) and acylation-deficient (Mut-YFP) 5-HT1A receptors after removing the stop codon (Fig. 1A). Immunoblot analysis performed in transfected neuroblastoma N1E-115 cells revealed a protein band with a predicted molecular mass of approximately 76 kDa for both WT-YFP and Mut-YFP constructs (Fig. 1B).

To exclude the possibility that fusion to the YFP alters receptor properties, we analyzed the subcellular distribution, pharmacological profile, and downstream signaling of the fluorescent-labeled receptors by comparison with the HA-tagged 5-HT1A receptors (Papoucheva et al., 2004). Cellular location of YFP-tagged receptors was first analyzed by the biotinylation assay. For that, intact cells expressing 5-HT1A receptors were labeled with a membrane-impermeable sulfo-NHS-biotin, and biotinylated proteins from plasma membranes were purified by streptavidin. Finally, receptors were revealed by immunoblotting using anti-HA or anti-GFP antibodies. As shown in Fig. 1C, both HA- and YFP-tagged 5-HT1A receptors were purified by streptavidin-agarose, suggesting that these receptors are expressed at the cell surface.

Confocal microscopy performed after transfection of WT-YFP or Mut-YFP constructs into N1E-115 cells also demonstrated that the major part of the YFP-tagged receptors was on the plasma membranes with only a minor fraction present in the intracellular compartments (Fig. 1D). The predominant localization of WT-YFP and Mut-YFP fusion proteins at the plasma membrane was also confirmed in transiently and in stably transfected NIH-3T3 cells (data not shown).

The pharmacological profiles of the WT-YFP and Mut-YFP constructs were analyzed by saturation binding of the selective 5-HT1A receptor agonist [^{3}H]8-OH-DPAT in the membrane preparations from transfected NIH-3T3 cells (Fig. 2A). The binding affinities of [^{3}H]8-OH-DPAT for WT-YFP (K_D = 0.72 ± 0.53 nM) and Mut-YFP (K_D = 0.97 ± 0.26 nM) were similar to that obtained for the HA-tagged receptors (K_D = 0.76 ± 0.23 nM). These values are also in accordance with those reported previously for recombinant and native 5-HT1A receptors (Newman-Tancredi et al., 1998; Pucadyil

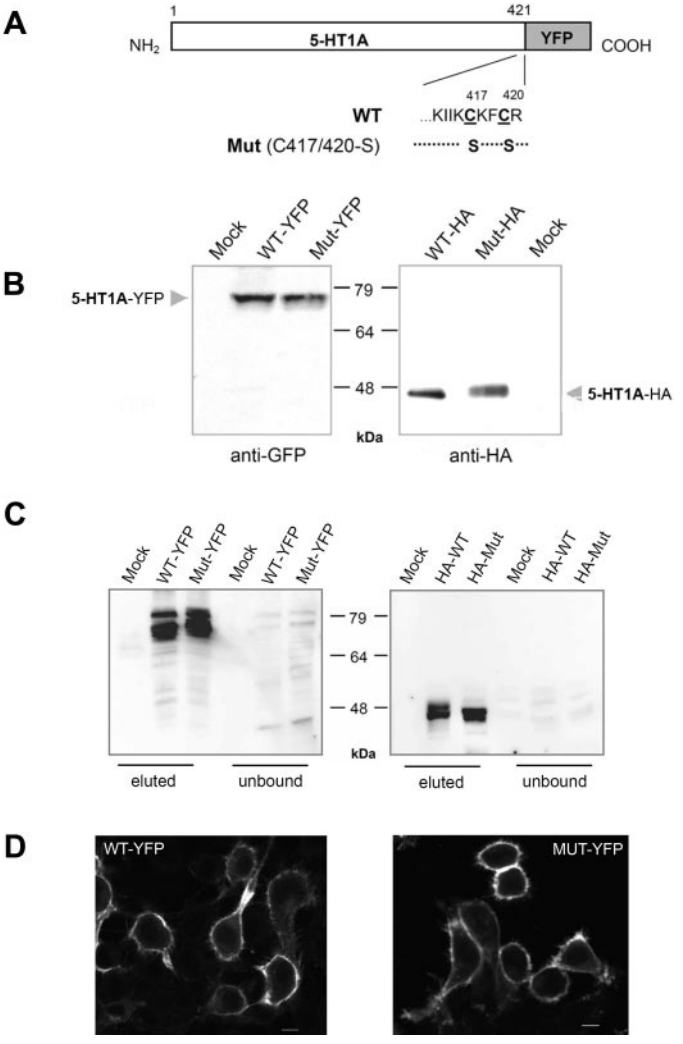

Fig. 1. Construction and expression of the YFP-tagged 5-HT1A receptors. A, schematic presentation of the wild-type and palmitoylation-deficient 5-HT1A receptors fused C-terminally with yellow fluorescent protein to produce WT-YFP and Mut-YFP constructs, respectively. C-terminal amino acid sequence of the 5-HT1A receptor is shown with a single-letter code. B, immunoblot analysis of YFP- and HA-tagged 5-HT1A receptors transiently expressed in N1E-115 cells. The blots were probed with antibodies directed against GFP- or HA-tag. The molecular mass marker is indicated between the panels. C, cell surface proteins were labeled with sulfo-NHS-biotin, and biotinylated proteins were isolated from the cell lysates with immobilized avidin. Biotinylated proteins were eluted and separated as described under *Materials and Methods*. Aliquots of unbound fractions and the eluates were analyzed by SDS-PAGE and immunoblotting with anti-HA (left) or anti-GFP (right) antibodies. Representative immunoblots are shown. D, intracellular distribution of WT-YFP and Mut-YFP constructs. Representative confocal images obtained with LSM510-Meta microscope at 63× magnification are shown. Scale bar, 10 μM.

et al., 2004), demonstrating that the YFP fusion does not change the receptor's pharmacological properties.

The ability of YFP-tagged receptors to stimulate G-protein activity was then analyzed by the fluorescence-based GTPγS assay performed on the membrane preparations from transfected N1E-115 cells in the presence or absence of 8-OH-DPAT. The binding specificity to the inhibitory G-proteins was provided by the immunoprecipitation of membrane preparations with anti-$G\alpha_{i3}$ antibody before the fluorescence measurement. As shown in Fig. 2B, activation of the HA-tagged receptor with 100 μM 8-OH-DPAT elicited an approximately 3.7-fold increase in [Eu]GTPγS binding. Activation of YFP-tagged 5-HT1A receptors resulted in the similar stimulation of GTPγS binding (Fig. 2B). In contrast, no stimulation of [Eu]GTPγS binding was observed in membranes of non-transfected cells (data not shown). When the ability of non-palmitoylated YFP-tagged 5-HT1A receptor mutant to stimulate [Eu]GTPγS binding was analyzed, we found that the relative activation of $G\alpha_{i3}$ subunit after agonist stimulation in this case was completely abolished (Fig. 2B). This was in line with our previous data obtained for acylation-deficient HA-tagged receptor (Papoucheva et al., 2004). It is also notable that treatment of HA- and YFP-tagged receptors with 8-OH-DPAT resulted in a dose-dependent increase of GTPγS binding to $G\alpha_{i3}$ proteins with very similar EC_{50} values (HA-WT, 1 ± 0.8 μM; WT-YFP, 3 ± 2 μM) (Fig. 2C). Parallel treatment of the membrane preparation from cells expressing YFP- or HA-tagged 5-HT1A receptors with the selective receptor antagonist WAY100635 at 1 μM concentration completely antagonized [Eu]GTPγS binding, indicating specific involvement of 5-HT1A in $G\alpha_i$ activation (Fig. 2C).

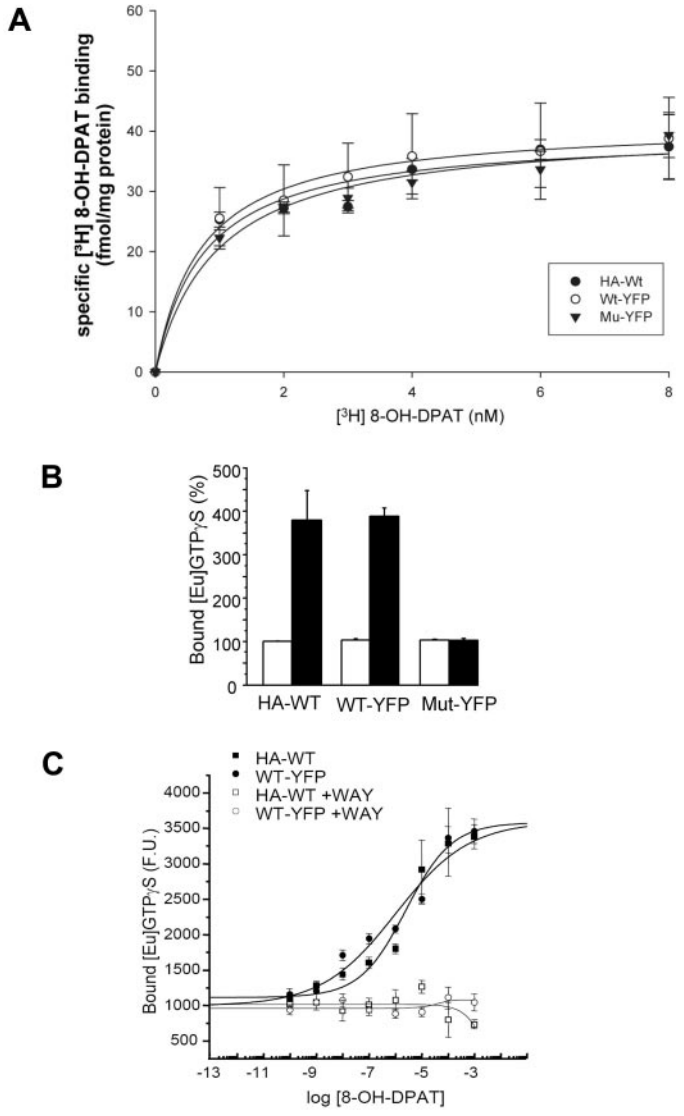

Fig. 2. Radioligand and [Eu]GTPγS binding studies of YFP-tagged 5-HT1A receptors. A, saturation binding analysis. The plots represent specific binding of agonist [³H]8-OH-DPAT to WT-YFP, Mut-YFP, and HA-WT. Radioligand binding assay was performed on membranes prepared from transfected NIH-3T3 cells. Data were fitted using the one-site saturation binding model, and data points represent the means ± S.E. from at least three independent experiments. B, the [Eu]GTPγS binding response for HA-WT, WT-YFP, and Mut-YFP was quantified at saturating concentration of 8-OH-DPAT (100 μM) and [Eu]GTPγS binding for HA-WT receptor in the absence of ligand was set as 100%. Each value represents the mean ± S.E. from three independent experiments. C, dose-response curves for ligand-induced $G\alpha_{i3}$-protein activation. [Eu]GTPγS binding to plasma membranes was measured with varying concentrations of 8-OH-DPAT after immunoprecipitation with anti-$G\alpha_{i3}$ antibody. In several experiments, WAY100635 (1 μM) was added to the membranes 5 min before agonist. Background fluorescence from non-transfected cells was substructed before the analysis. Data points represent the means ± S.E. from three independent experiments. F.U., fluorescence units.

Monitoring 5-HT1A-Mediated Calcium Signaling in Living Cells. The 5-HT1A receptor has been shown to activate phospholipase C-mediated Ca^{2+} release from the intracellular stores via Gβγ subunits both in transfected and in cells endogenously expressing 5-HT1A (Liu and Albert, 1991; Aune et al., 1993; Pauwels and Colpaert, 2003). Therefore, functional coupling of WT-YFP and Mut-YFP receptors to calcium mobilization was examined by monitoring $[Ca^{2+}]_i$ in transiently transfected in N1E-115 cells loaded with the fluorescent calcium chelator Fura-2/AM. In addition to the receptors, cells were cotransfected with the functional $G\alpha_{i3}$-CFP fusion protein (Leaney et al., 2002), which is resistant to the pertussis toxin (PTx), and treated with PTx to avoid the receptor-dependent activation of endogenous G_i-proteins.

When the cells were transfected with recombinant $G\alpha_{i3}$-CFP protein in the absence of exogenous 5-HT1A receptor, no Ca^{2+} response was obtained after treatment of the cells with 8-OH-DPAT (Fig. 4A). Similar results were observed when $G\alpha_{i3}$-CFP was coexpressed with the 5-HT7-YFP receptor (data not shown). In contrast, coexpression of WT-YFP recep-

tor with $G\alpha_{i3}$-CFP significantly increased fluorescence ratio F/F_0 upon stimulation with 8-OH-DPAT, reflecting an increase in $[Ca^{2+}]_i$ (Fig. 4B). Treatment of the cotransfected cells with the selective 5-HT1A receptor antagonist WAY100635 at 1 μM concentration blocked this effect, indicating that the increase in the Ca^{2+} concentration was specifically mediated by 5-HT1A receptor activation (Fig. 4C). It is noteworthy that coexpression of the Mut-YFP receptor with $G\alpha_{i3}$-CFP did not produce any significant changes in the Ca^{2+} response after receptor stimulation with agonist (Fig. 4D).

5-HT1A-Mediated Redistribution of $G\alpha_i$-Proteins in Living Cells. To study subcellular distribution of 5-HT1A-mediated signaling in real time, N1E-115 cells were transfected with the 5-HT1A-YFP receptors together with the functional $G\alpha_{i3}$-CFP fusion protein (Leaney et al., 2002). The $G\alpha_{i3}$-CFP protein also contains a C-terminal C-I mutation providing its resistance to the PTx. Coupling of the 5-HT1A receptor with endogenous $G_{i/o}$-proteins was disabled by treatment of transfected cells with PTx. Confocal microscopy of living cells revealed that both $G\alpha_{i3}$-CFP and 5-HT1A-YFP constructs were primarily distributed on the plasma membrane, where they were partly colocalized (Fig. 5, A and B).

As shown in Fig. 5A, treatment of cells expressing the WT-YFP receptor with 8-OH-DPAT results in a redistribution of the $G\alpha_{i3}$-CFP from the plasma membrane to the cytoplasm. Quantitative image analysis performed on the *z*-stack projections revealed approximately 2.5-fold increase in the fluorescence intensity ratio $\Delta F/F_0$ for the $G\alpha_{i3}$-CFP within the cytoplasm in response to the agonist stimulation (Fig. 5C). In contrast, the fluorescence of the WT-YFP receptor was not significantly redistributed upon agonist stimulation (Fig. 5A). The receptor-dependent translocation of the $G\alpha_{i3}$-CFP was obtained in approximately 30% of transfected cells, indicating the importance of a proper stoichiometry between the signaling components. The agonist-dependent internalization of $G\alpha_{i3}$-CFP was specifically mediated by the 5-HT1A receptor, because it was blocked by the receptor specific antagonist WAY100635 (data not shown). Moreover, the agonist-dependent redistribution of the $G\alpha_{i3}$-CFP was not obtained in the absence of WT-YFP or in cells expressing YFP-tagged 5-HT7 receptor, which is known to activate stimulatory G_s-protein in response to 8-OH-DPAT (data not shown).

When acylation-deficient receptor mutant (Mut-YFP) was coexpressed together with $G\alpha_{i3}$-CFP in N1E-115 cells, their

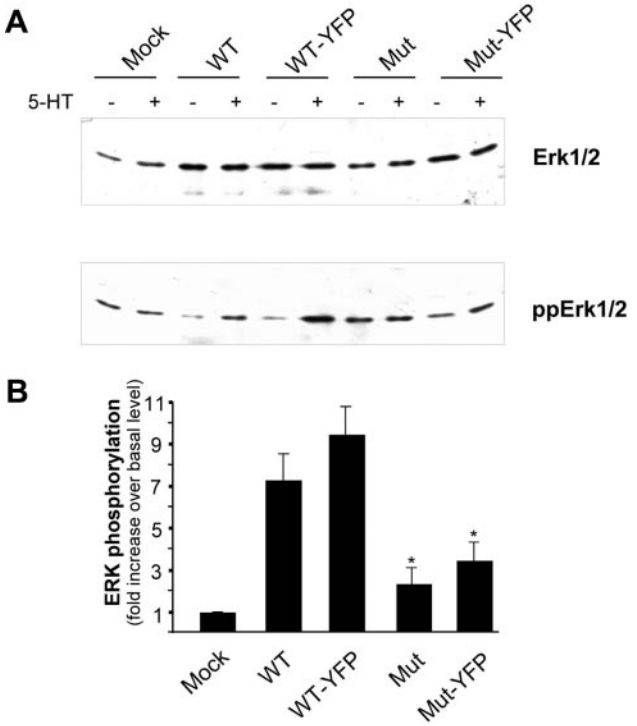

Fig. 3. Activation of Erk by YFP-tagged 5-HT1A receptors. A, NIH-3T3 cells expressing YFP- or HA-tagged 5-HT1A receptors were treated for 5 min with 10 μM 8-OH-DPAT or vehicle, separated by SDS-PAGE, and then subjected to immunoblot either with antibodies raised against total (top) or phosphorylated (bottom) Erk. Fluorograms are representative of three independent experiments. B, quantification of Erk phosphorylation was performed by densitometry and calculated as the ratio of total Erk expression over the Erk phosphorylation signal. Each value represents the mean ± S.E. (n = 3). A statistically significant difference between values is noted (*, $p < 0.05$).

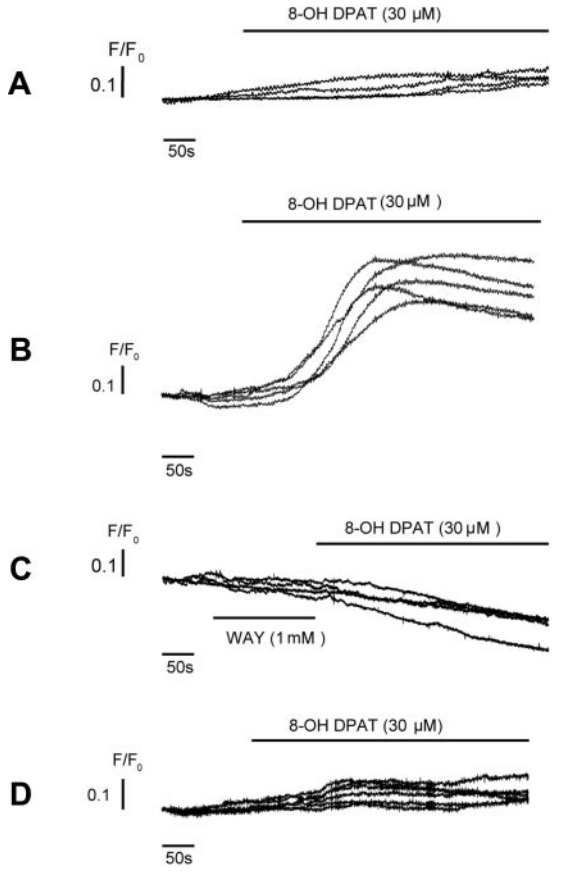

Fig. 4. 5-HT1A receptor-mediated changes in intracellular Ca^{2+} concentration. Neuroblastoma N1E-115 cells were transiently transfected with YFP-tagged 5-HT1A receptors and $G\alpha_{i3}$-CFP construct. Changes in $[Ca^{2+}]_i$ were measured using calcium indicator FURA-2/AM. Cells coexpressing YFP-tagged receptor and $G\alpha_{i3}$-CFP were selected by fluorescence microscopy with appropriate excitation and emission filter sets. Activity of endogenous G_i-proteins was blocked by the overnight pretreatment of cells with PTx (100 ng/ml). Data are representative of four independent experiments, and every trace corresponds to one measured cell. A, Ca^{2+} response in N1E-115 cells transfected with $G_{i3}\alpha$-CFP construct alone. B, cells coexpressing WT-YFP and $G\alpha_{i3}$-CFP showed increase in intracellular Ca^{2+} concentration after stimulation of receptor with 8-OH-DPAT. C, pretreatment of cells cotransfected with $G\alpha_{i3}$-CFP and WT-YFP constructs with 5-HT1A antagonist WAY100635 blocked 8-OH-DPAT-induced Ca^{2+} response. D, in cells expressing acylation-deficient Mut-YFP receptor together with the $G\alpha_{i3}$-CFP, no increase in $[Ca^{2+}]_i$ was induced upon receptor stimulation.

intracellular distribution was similar to that obtained for the cells cotransfected with WT-YFP receptor. However, there were no significant changes in localization of $G\alpha_{i3}$-CFP after stimulation of cells with 5-HT1A agonist 8-OH-DPAT (Fig. 5, B and C).

To further examine the activation-dependent distribution of $G\alpha_i$, cellular fractionation of N1E-115 cells expressing either WT-YFP or Mut-YFP in addition to the $G\alpha_{i3}$-CFP was performed. The $G\alpha_{i3}$-CFP was visualized by immunoblotting of transfected and PTx-treated cells with antibody directed against $G\alpha_i$-subunits, which allows parallel detection of endogenous $G\alpha_i$-proteins. Immunoblot analysis reveals that 8-OH-DPAT activation of the WT-YFP receptor causes a shift of $G\alpha_{i3}$-CFP from the particulate to the soluble fraction. In contrast, stimulation of the acylation-deficient, YFP-tagged receptor does not result in change of $G\alpha_{i3}$-CFP solubility (Fig. 5D). It is also notable that there was some translocation of the endogenous $G\alpha_i$ proteins after receptor stimulation. These combined results demonstrate that stimulation of the 5-HT1A receptor leads to the translocation of $G\alpha_i$-subunits from the membrane to the cytoplasm, and that receptor palmitoylation is critically involved in the regulation of this event.

Distribution of WT and Palmitoylation-Deficient 5-HT1A Receptors within Membrane Subdomains (Gradient Centrifugation). Lipid modifications have been shown to play a role in the partitioning of several proteins into defined membrane subdomains, like lipid rafts and caveolae (Arni et al., 1998; Melkonian et al., 1999; Moffett et al., 2000). To determine, whether this may be the case for the 5-HT1A receptor, we compared the membrane distribution of the wild-type receptor and acylation-deficient mutant using density gradient centrifugation. To avoid artifacts resulting from overexpression, we generated NIH-3T3 cell lines stably

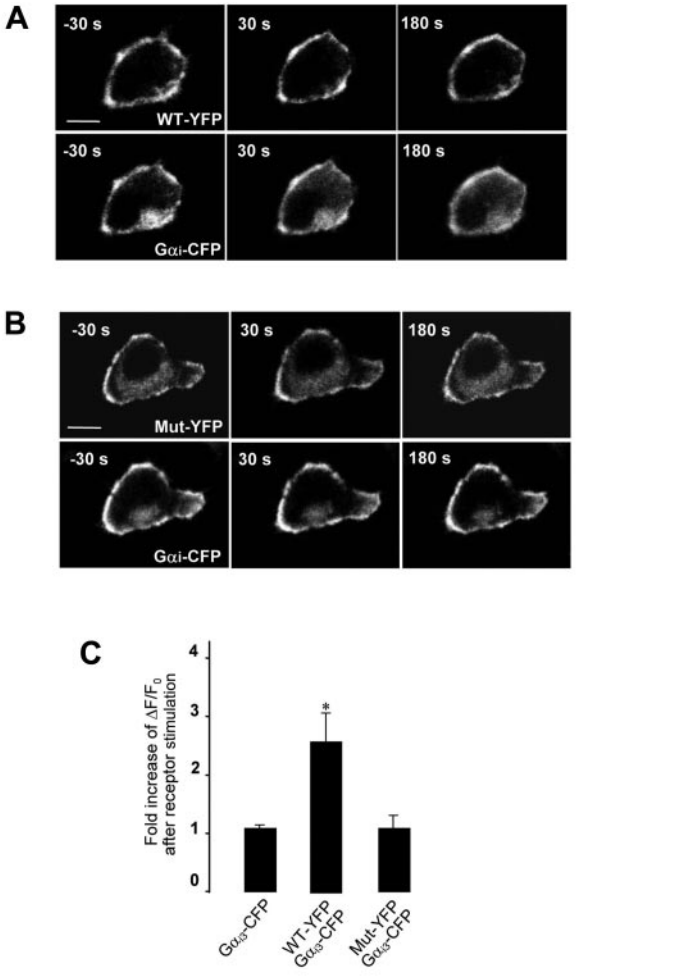

Fig. 5. Translocation of $G\alpha_{i3}$-CFP fusion protein in the living N1E-115 cells upon activation of the 5-HT1A receptor. Cells were cotransfected with $G\alpha_{i3}$-CFP protein and with either WT-YFP or Mut-YFP receptors and viewed by confocal microscopy. To block coupling of receptor to endogenous G_i-proteins, cells were treated with pertussis toxin. Images were assembled at 10-s intervals, and the specific 5-HT1A receptor agonist 8-OH-DPAT was added at time point 0. Representative confocal images obtained with LSM510-Meta at magnification of 63× are shown for cells expressing WT-YFP receptor together with $G\alpha_{i3}$-CFP (A) or acylation-deficient Mut-YFP construct together with $G\alpha_{i3}$-CFP (B). Scale bar, 10 μm. C, quantitative image analysis of cells before and during treatment with 8-OH-DPAT. Changes in CFP fluorescence intensity within the cytoplasm were calculated as described under *Materials and Methods.* A statistically significant difference between values is noted (**, $p < 0.01$). Each value represents the mean ± S.E. from at least three independent experiments. D, cellular fractionation of N1E-115 cells expressing either WT-YFP or Mut-YFP together with $G\alpha_{i3}$-CFP. Activity of endogenous G_i-proteins was blocked by pretreatment of cells with PTx. Transfection cells were treated with 8-OH-DPAT for 30 s, rapidly harvested, and the content of $G\alpha_{i3}$-CFP (top) and endogenous $G\alpha_{i3}$ (bottom) in soluble and membrane fractions was examined by immunoblot analysis.

expressing low amounts of WT-YFP (304 ± 62 fmol/mg) or Mut-YFP (605 ± 64 fmol/mg). These cells were solubilized in ice-cold Triton X-100 and subjected to centrifugation in Optiprep density gradient to isolate detergent-insoluble membrane fractions. Immunoblot analysis of gradient fractions revealed that 33 ± 11% (n = 4) of the wild-type 5-HT1A receptor floated with the detergent-resistant low-density fractions along with the caveolae-specific protein caveolin-1 and the α_{i3} subunit of heterotrimeric G-protein (Fig. 6, A and C). When the NIH-3T3 cells stably expressing Mut-YFP were analyzed, the yield of palmitoylation-deficient receptor in the light Triton X-100-resistant membrane fraction was reduced to 4 ± 3% (n = 4; Fig. 6, B and C). It is also notable that distribution of the raft and nonraft markers did not change in cells expressing Mut-YFP compared with the corresponding fractions generated from the WT-YFP expressing cells (Fig. 6D). Similar highly reproducible distribution patterns were also obtained in CHO cells transiently transfected with HA-tagged wild-type or acylation-deficient 5-HT1A receptors (data not shown). This suggests that palmitoylation represents a targeting signal responsible for the partial localization of the 5-HT1A receptor in lipid rafts. This assumption was further supported by the observation that the pretreatment of cells with methyl-β-cyclodextrin (MβCD) significantly reduced the amount of WT-YFP receptor and $G\alpha_{i3}$-subunit in the low-density fractions (Fig. 7). The cholesterol-binding reagent MβCD was shown previously to disrupt the cholesterol-enriched membrane subdomains by depletion of cholesterol from the plasma membrane (Harder et al., 1998).

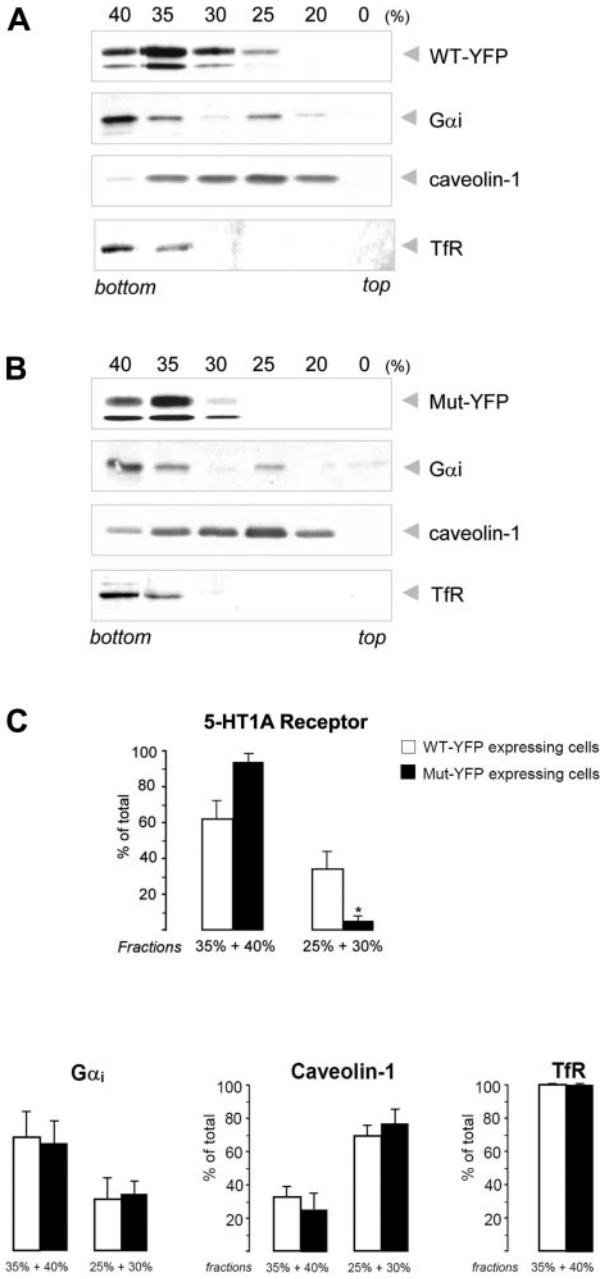

Fig. 6. Localization of the wild-type and acylation-deficient 5-HT1A receptors in the DRMs. The NIH-3T3 cells stably expressing either the WT-YFP (A) or the Mut-YFP (B) were lysed with the cold 1% Triton X-100, and lysates were ultracentrifuged in the Optiprep density gradient. The gradient fractions were analyzed by immunoblotting. $G\alpha_i$ protein and caveolin-1 were used as DRM markers, whereas transferrin receptor (TfR) was used as the non-DRM marker. C, relative amount of the receptor in the high-density fractions (35% + 40%) and the buoyant low-density fractions (25% + 30%). Quantitative analysis of the receptor distribution was performed by densitometry and calculated in percentage of the total protein amount in all fractions. Data points represent mean ± S.E. (n = 4). A statistically significant difference between values is noted (*, $p < 0.05$). D, relative amount of the caveolin-1, $G\alpha_i$, and transferrin receptor (TfR) in the high-density fractions (35% + 40%) and the buoyant low-density fractions (25% + 30%). Data points represent mean ± S.E. (n = 3).

Distribution of WT and Palmitoylation-Deficient 5-HT1A Receptors within Membrane Subdomains (Copatching of the 5-HT1A Receptor with Raft Marker GM1). In addition to the gradient centrifugation experiments, we used fluorescence microscopy techniques to analyze the association of 5-HT1A receptor with lipid rafts on native plasma membrane sheets by using a copatching assay (Harder et al., 1998). Membrane sheets from the stably transfected NIH-3T3 cells were prepared by a brief ultrasound pulse, leaving behind the basal plasma membrane attached to the glass coverslip (Lang et al., 2001). After fixation of membrane sheets, lipid rafts were visualized by treatment with CTX, which binds to the raft-associated gan-

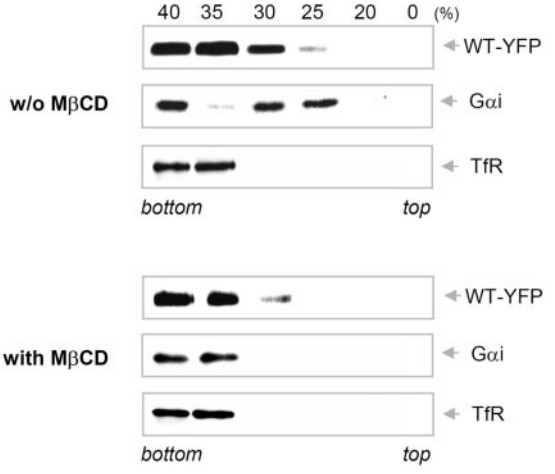

Fig. 7. Cholesterol depletion reduces localization of the WT-YFP and the $G\alpha_i$ in the DRMs. The NIH-3T3 cells (1×10^6) stably expressing the WT-YFP were treated with 10 mM MβCD for 45 min or were left untreated (w/o MβCD), lysed with cold 1% Triton X-100, and subjected to the ultracentrifugation in the Optiprep density gradient. The gradient fractions were analyzed by SDS-PAGE and immunoblotting. Representative fluorogram is shown (n = 3).

glioside GM1. As shown in Fig. 8A (a to d), both GM1 and 5-HT1A-YFP receptor signals were highly abundant and relative homogenous, thus not allowing to differentiate between specific and random colocalization. Therefore, segregation of the lipid rafts and receptors in more distinct domains was induced by incubating the *native* versus *fixed* membrane sheets with low concentrations of CTX and an anti-GFP antibody, respectively, to cross-link the corresponding domains (Spiegel et al., 1984). Such treatment resulted in the concentration of both labels in less numerous and clearly defined spots that were scattered over the membrane surface (Fig. 8A; e to l). It is also noteworthy that the depletion of cholesterol by treatment of the intact membrane sheets with MβCD resulted in a more homogenous distribution of both receptor and GM1 fluorescence (Fig. 9). A similar distribution was also obtained in the absence of the cross-linking reagents (Fig. 9).

A detailed analysis of the 5-HT1A receptor and GM1-derived fluorescence patterns revealed that 30.3 ± 4.1% (n = 3; in every repetition at least 10 different sheets were analyzed) of the wild-type receptor patches were also enriched with the lipid raft marker GM1. It is noteworthy that this value was 3-fold reduced for the acylation-deficient mutant (Fig. 8, B and C). These data demonstrate that a fraction of the 5-HT1A receptor is associated with the lipid rafts. These findings are also in line with the gradient centrifugation data suggesting the importance of palmitoylation for localization of the 5-HT1A receptor in the lipid rafts.

Discussion

The convenience of GFP labeling in combination with the recent advances in imaging techniques has allowed for not only qualitative but also quantitative analysis of protein localization, trafficking, and mobility in living cells (Chudakov et al., 2005). More specifically, fluorescence labeling of GPCRs represents a powerful tool for direct visualization of receptor-mediated signaling in real time (Kallal and Benovic, 2000; Milligan, 2004). In the present study, we used YFP-tagged 5-HT1A receptor wild-type (WT-YFP) and its acylation-deficient mutant (Mut-YFP) to analyze their subcellular dynamics and to elucidate the role of receptor palmitoylation. Functionality of receptor-YFP constructs was assessed by the analysis of their subcellular distribution and by pharmacological studies. In addition, the efficiency of downstream signaling was tested by GTPγS binding assay and by receptor-dependent activation of extracellular signal-regulated kinases and Ca^{2+} release. In all cases, YFP-chimera demonstrated responses similar to their nonfluorescent wild-type or acylation-deficient counterparts, indicating that YFP-fused receptors can be used in functional studies.

Dynamics of 5-HT1A-Mediated Signaling. Because the components of the GPCR signaling cascade are expressed at

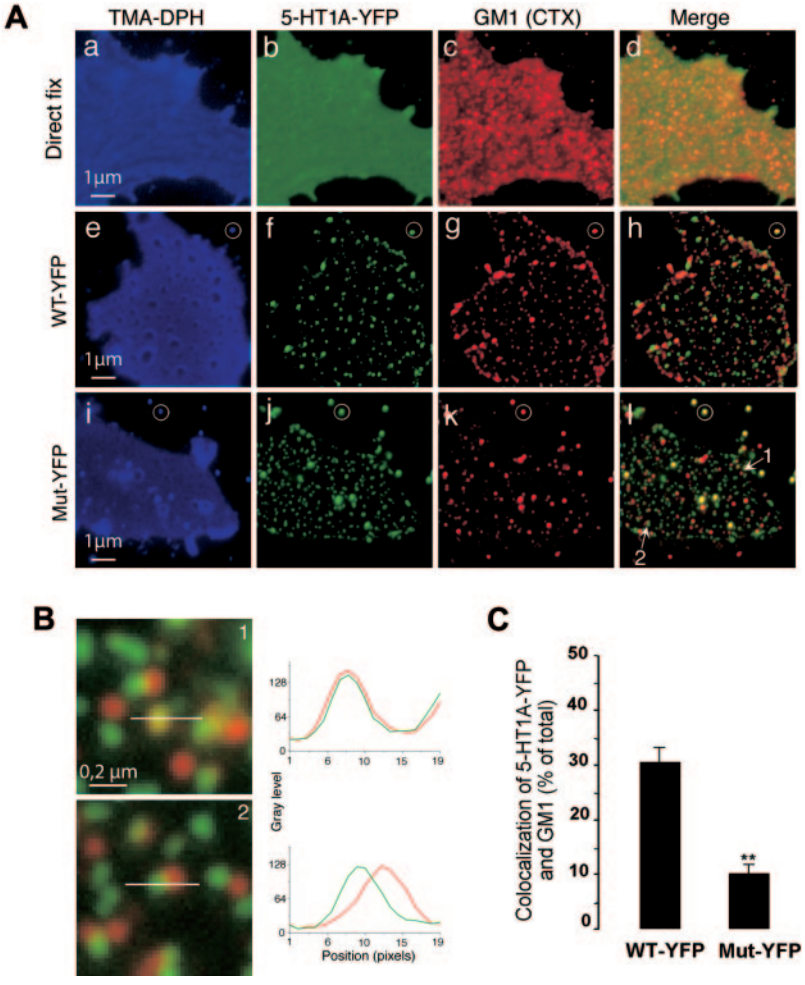

Fig. 8. Copatching of WT-YFP and Mut-YFP receptors with lipid raft ganglioside GM1. A, copatching assay was performed in plasma membrane sheets derived from the stably transfected NIH-3T3 cells. a, e, and i, staining of the membrane lipids with TMA-DPH (*blue*). b, f, and j, copatching of 5-HT1A-YFP receptors with anti-GFP antibody (green). c, g, and l, copatching of GM1 with cholera toxin. GM1 patches were detected using Alexa546 anti-CTX antibody (red). d, h, and k, the merge of receptor and GM1 signals. a to d, membrane sheets were fixed before incubation with anti-GFP antibody and CTX. e to l, membrane sheets were fixed after incubation with anti-GFP antibody and CTX. Circles mark the fluorescent beads that were used to align images obtained in different fluorescence channels for quantitative analysis. B, example of the line scans analysis for regions 1 and 2, which are shown with arrows in l. Fluorescence intensity was analyzed pixel by pixel along the line applied on the merge pictures. When the distance between the maximal values obtained for green and red fluorescence was less than 2 pixels, a colocalization event was counted (top). Otherwise, patches were counted as noncolocalized (bottom). C, quantitative analysis of colocalization events between WT-YFP or Mut-YFP and GM1. Data points represent mean ± S.E. (n = 3). A statistically significant difference between values is noted (**, $p < 0.01$).

relatively low concentration (Alousi et al., 1991; Milligan, 1996; Ostrom et al., 2000), their spatiotemporal organization and activation-dependent dynamics are crucial determinants regulating the specificity and potency of signaling pathways. (Hur and Kim, 2002). In the present study, we analyzed the dynamic distribution of the serotonin-mediated signaling using YFP-fused 5-HT1A receptors and the functional $G\alpha_{i3}$-CFP protein (Leaney et al., 2002). Time-lapse microscopy experiments demonstrated that in cells coexpressing WT-YFP and $G\alpha_{i3}$-CFP, receptor stimulation resulted in translocation of the $G\alpha_{i3}$-CFP from the plasma membrane to the cytoplasm. This observation was also consistent with cell fractionation experiments, demonstrating an activation-induced shift of $G\alpha_{i3}$-CFP to the soluble fraction. These results extend previous data obtained with stimulatory $G\alpha_s$-protein, for which activation-mediated relocation from the particular to the soluble fraction has been demonstrated (Levis and Bourne, 1992; Wedegaertner et al., 1996). Such activation-dependent translocation of stimulatory $G\alpha_s$-subunit was recently directly confirmed by using functional $G\alpha_s$-GFP fusion protein (Yu and Rasenick, 2002). Although true for $G\alpha_s$ and, as shown in the present study, for $G\alpha_{i/o}$ proteins, activation-mediated translocation of $G\alpha$-subunits seems to not be a general phenomenon. Experiments with $G\alpha_q$ revealed that this G-protein is stably associated with the plasma membrane, and agonist stimulation did not evoke its relocation (Hughes et al., 2001). One possible explanation for such discrepancies could be a different distribution of these G-proteins at the cell surface: G_i- and G_s-proteins have been shown to specifically concentrate in lipid raft domains, whereas G_q preferentially accumulates in caveolae via its specific interaction with caveolin (Oh and Schnitzer, 2001).

Palmitoylation and Localization of the 5-HT1A Receptor in Lipid Microdomains. We have demonstrated previously that the 5-HT1A receptor is palmitoylated at its C-terminal cysteine residues Cys417 and Cys420. Characterization of acylation-deficient 5-HT1A mutants revealed the importance of receptor palmitoylation for signaling (Papoucheva et al., 2004). However, molecular mechanisms by which palmitoylation may regulate receptor-dependent G-protein activation are still unknown. One possibility could be the involvement of 5-HT1A receptor palmitoylation in trafficking and/or localization of the receptor into specific membrane subdomains, like lipid rafts.

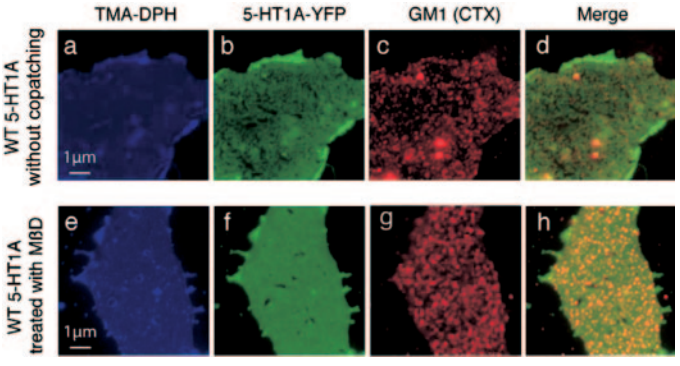

Fig. 9. a to d, distribution of WT-YFP and ganglioside GM1 in the membrane sheets in the absence of the cross-linking reagents. Copatching assay was performed on fixed plasma membrane sheets derived from the stably transfected NIH-3T3 cells after 60 min of incubation in KGlu buffer at 37°C without antibodies and without the cholera toxin. e to h, distribution of WT-YFP and ganglioside GM1 after cholesterol depletion with methyl-β-dextran. Methyl-β-dextran was applied at 5 mM concentration for 10 min, and copatching was performed as described under *Materials and Methods*. a and e, staining of the membrane lipids with TMA-DPH. b and f, copatching of 5-HT1A-YFP receptors with anti-GFP antibody. c and g, copatching of GM1 with cholera toxin. GM1 patches were detected using Alexa546-labeled anti-CTX antibody. d and h, the merge of receptor and GM1 signals.

Protein modification by the covalent attachment of saturated fatty acyl chains, including myristic and palmitic acids, represents one of the best characterized lipid raft targeting signals (Moffett et al., 2000; Zacharias et al., 2002). The long-chain fatty acids are expected to pack well in the l_o phase, increasing the avidity of protein for sphingolipid/cholesterol-enriched domains (Melkonian et al., 1999). Therefore, a number of acylated proteins, including heterotrimeric G-proteins α subunits, some Src family kinases, and growth-associated protein 43, that are resident in the lipid rafts (Arni et al., 1998; Melkonian et al., 1999; Moffett et al., 2000). It has been also shown that removal of the fatty acid modifications leads to the loss of the protein association with lipid rafts and caveolae (Shenoy-Scaria et al., 1994; Shaul et al., 1996; Song et al., 1997; Moffett et al., 2000). It is, however, noteworthy that the described results were mainly obtained with peripheral membrane proteins and cannot be simply extended to integral membrane proteins. The role of palmitoylation as a raft targeting signal for the latter remains controversial. For example, it has been shown that mutation of all palmitoylated cysteine residues on caveolin-1 does not affect its caveolae localization (Dietzen et al., 1995). On the other hand, reconstitution experiments have demonstrated that defined transmembrane peptides become excluded from l_o domains regardless of their acylation state (van Duyl et al., 2002). For the GPCRs whose C-terminal intracellular domains are often palmitoylated, the role of acylation as a targeting signal for the rafts/caveolae localization has not been investigated so far. Several members of the GPCR superfamily have been shown to be highly enriched in lipid rafts and caveolae, whereas others are present only in small amounts or are excluded from the lipid rafts (Chini and Parenti, 2004).

In the present study, we found that approximately 33% of the wild-type 5-HT1A receptor resides in the DRMs. Cholesterol depletion results in solubilization of the 5-HT1A receptor, confirming association of the receptor with the cholesterol-enriched domains. DRM localization of the 5-HT1A was equally evident in different cell types (NIH-3T3 and CHO), suggesting that segregation of the receptor into lipid subdomains is intrinsic to the 5-HT1A itself. In contrast to the wild-type receptor, the amount of acylation-deficient 5-HT1A receptor residing in Triton X-100-insoluble fractions was significantly reduced, suggesting a functional involvement of receptor palmitoylation for the DRM trafficking.

Treatment of cells with nonionic detergents at low temperature used in this study represents a classic approach for the DRM isolation. However, this method often produces controversial results and should not be expected to extract lipid rafts from cell membranes precisely (Simons and Vaz, 2004). Therefore, we used copatching as an additional assay to analyze the membrane distribution of the 5-HT1A receptor. This assay is based on the observation that two membrane components sharing a preference for lipid rafts will coalesce to form tightly associated patches after treatment with specific cross-linking reagents, like antibodies or multimeric

toxins (Harder et al., 1998). Analysis of copatching data revealed that 30.3 ± 4.1% of the 5-HT1A receptor was colocalized with the lipid raft ganglioside GM1. In contrast, the colocalization of the acylation-deficient mutant with the raft marker was drastically reduced. Thus, by using two independent methods, we demonstrated that the significant fraction of the 5-HT1A receptor resides in lipid rafts in a palmitoylation-dependent manner, demonstrating that stable palmitoylation of the 5-HT1A receptor represents an important targeting signal responsible for the localization of receptor in GM1-enriched membrane subdomains. Combined with our previous data on the signaling deficiency of nonpalmitoylated 5-HT1A receptor, this finding also suggests that the palmitoylation-dependent raft localization of the receptor is involved in the regulation of signaling processes.

How can palmitoylation-mediated localization of the 5-HT1A receptor in rafts be involved in the regulation of receptor activity? One possible scenario is that the irreversible receptor palmitoylation will accelerate the transient targeting of the receptor to lipid rafts. Such transient raft association may be further stabilized by the precoupling of the receptor with the $G\alpha_i$ protein (Emerit et al., 1990), which mainly resides in rafts (Oh and Schnitzer, 2001). Activation of the receptor will result in dissociation of the receptor-bound G_i-protein heterotrimeric complex, thereby reducing the fraction of receptor interacting with G-protein (Janetopoulos et al., 2001). Such uncoupled receptors have been shown to possess increased mobility (Pucadyil et al., 2004) and could therefore leave the lipid microdomains by lateral diffusion. Outside of lipid rafts, the uncoupled 5-HT1A receptors become partly "nonfunctional" in terms of efficient signaling and need to undergo another cycle of raft localization to initialize activation of the G_i-protein and downstream effectors upon stimulation. Several experimental observations support this model: 1) our data demonstrate that nonfunctional, acylation-deficient 5-HT1A mutant is excluded from DRMs; 2) removal of cholesterol from hippocampal cells has been found to affect G_i-protein coupling of the 5-HT1A receptor and to affect the specific agonist binding (Pucadyil and Chattopadhyay, 2004); and 3) it has been shown that differently to other GPCRs, prolonged agonist stimulation of the 5-HT1A receptor does not result in considerable receptor internalization (Riad et al., 2001; Pucadyil et al., 2004).

Acknowledgments

We thank Dr. Michael F. G. Schmidt for valuable discussions and suggestions regarding the manuscript.

References

Alousi AA, Jasper JR, Insel PA, and Motulsky HJ (1991) Stoichiometry of receptor-Gs-adenylate cyclase interactions. *FASEB J* **5:**2300–2303.
Anderson RG (1998) The caveolae membrane system. *Annu Rev Biochem* **67:**199–225.
Andrade R, Malenka RC, and Nicoll RA (1986) A G protein couples serotonin and GABAB receptors to the same channels in hippocampus. *Science* **234:**1261–1265.
Arni S, Keilbaugh SA, Ostermeyer AG, and Brown DA (1998) Association of GAP-43 with detergent-resistant membranes requires two palmitoylated cysteine residues. *J Biol Chem* **273:**28478–28485.
Aune TM, McGrath KM, Sarr T, Bombara MP, and Kelley KA (1993) Expression of 5HT1a receptors on activated human T cells. Regulation of cyclic AMP levels and T cell proliferation by 5-hydroxytryptamine. *J Immunol* **151:**1175–1183.
Avery J, Ellis DJ, Lang T, Holroyd P, Riedel D, Henderson RM, Edwardson JM, and Jahn R (2000) A cell-free system for regulated exocytosis in PC12 cells. *J Cell Biol* **148:**317–324.
Brown DA and London E (1998) Functions of lipid rafts in biological membranes. *Annu Rev Cell Dev Biol* **14:**111–136.
Burnet PW, Mefford IN, Smith CC, Gold PW and Sternberg EM (1996) Hippocampal 5-HT1A receptor binding site densities, 5-HT1A receptor messenger ribonucleic acid abundance and serotonin levels parallel the activity of the hypothalamo-pituitary-adrenal axis in rats. *Behav Brain Res* **73:**365–368.
Chini B, and Parenti M (2004) G-protein coupled receptors in lipid rafts and caveolae: how, when and why do they go there? *J Mol Endocrinol* **32:**325–338.
Chudakov DM, Lukyanov S, and Lukyanov KA (2005) Fluorescent proteins as a toolkit for in vivo imaging. *Trends Biotechnol* **23:**605–613.
Claeysen S, Sebben M, Becamel C, Bockaert J, and Dumuis A (1999) Novel brain-specific 5-HT4 receptor splice variants show marked constitutive activity: role of the C-terminal intracellular domain. *Mol Pharmacol* **55:**910–920.
Cowen DS, Sowers RS, and Manning DR (1996) Activation of a mitogen-activated protein kinase (ERK2) by the 5-hydroxytryptamine1A receptor is sensitive not only to inhibitors of phosphatidylinositol 3-kinase, but to an inhibitor of phosphatidylcholine hydrolysis. *J Biol Chem* **271:**22297–22300.
De Vivo M and Maayani S (1986) Characterization of the 5-hydroxytryptamine1a receptor-mediated inhibition of forskolin-stimulated adenylate cyclase activity in guinea pig and rat hippocampal membranes. *J Pharmacol Exp Ther* **238:**248–253.
Dietzen DJ, Hastings WR, and Lublin DM (1995) Caveolin is palmitoylated on multiple cysteine residues. Palmitoylation is not necessary for localization of caveolin to caveolae. *J Biol Chem* **270:**6838–6842.
Dumuis A, Sebben M, and Bockaert J (1988) Pharmacology of 5-hydroxytryptamine-1A receptors which inhibit cAMP production in hippocampal and cortical neurons in primary culture. *Mol Pharmacol* **33:**178–186.
Emerit MB, el Mestikawy S, Gozlan H, Rouot B, and Hamon M (1990) Physical evidence of the coupling of solubilized 5-HT1A binding sites with G regulatory proteins. *Biochem Pharmacol* **39:**7–18.
Eroglu C, Brugger B, Wieland F, and Sinning I (2003) Glutamate-binding affinity of *Drosophila* metabotropic glutamate receptor is modulated by association with lipid rafts. *Proc Natl Acad Sci U S A* **100:**10219–10224.
Fargin A, Yamamoto K, Cotecchia S, Goldsmith PK, Spiegel AM, Lapetina EG, Caron MG, and Lefkowitz RJ (1991) Dual coupling of the cloned 5-HT1A receptor to both adenylyl cyclase and phospholipase C is mediated via the same Gi protein. *Cell Signal* **3:**547–557.
Foster LJ, De Hoog CL, and Mann M (2003) Unbiased quantitative proteomics of lipid rafts reveals high specificity for signaling factors. *Proc Natl Acad Sci U S A* **100:**5813–5818.
Garnovskaya MN, van Biesen T, Hawe B, Casanas Ramos S, Lefkowitz RJ, and Raymond JR (1996) Ras-dependent activation of fibroblast mitogen-activated protein kinase by 5-HT1A receptor via a G protein beta gamma-subunit-initiated pathway. *Biochemistry* **35:**13716–13722.
Gordon JA and Hen R (2004) The serotonergic system and anxiety. *Neuromol Med* **5:**27–40.
Harder T, Scheiffele P, Verkade P, and Simons K (1998) Lipid domain structure of the plasma membrane revealed by patching of membrane components. *J Cell Biol* **141:**929–942.
Hughes TE, Zhang H, Logothetis DE, and Berlot CH (2001) Visualization of a functional $G\alpha_q$-green fluorescent protein fusion in living cells. Association with the plasma membrane is disrupted by mutational activation and by elimination of palmitoylation sites, but not be activation mediated by receptors or AlF4. *J Biol Chem* **276:**4227–4235.
Hur EM and Kim KT (2002) G protein-coupled receptor signalling and cross-talk: achieving rapidity and specificity. *Cell Signal* **14:**397–405.
Janetopoulos C, Jin T, and Devreotes P (2001) Receptor-mediated activation of heterotrimeric G-proteins in living cells. *Science* **291:**2408–2411.
Kallal L and Benovic JL (2000) Using green fluorescent proteins to study G-protein-coupled receptor localization and trafficking. *Trends Pharmacol Sci* **21:**175–180.
Lang T, Bruns D, Wenzel D, Riedel D, Holroyd P, Thiele C, and Jahn R (2001) SNAREs are concentrated in cholesterol-dependent clusters that define docking and fusion sites for exocytosis. *EMBO J* **20:**2202–2213.
Leaney JL, Benians A, Graves FM, and Tinker A (2002) A novel strategy to engineer functional fluorescent inhibitory G-protein α subunits. *J Biol Chem* **277:**28803–28809.
Levis MJ and Bourne HR (1992) Activation of the alpha subunit of Gs in intact cells alters its abundance, rate of degradation, and membrane avidity. *J Cell Biol* **119:**1297–1307.
Liu YF and Albert PR (1991) Cell-specific signaling of the 5-HT1A receptor. Modulation by protein kinases C and A. *J Biol Chem* **266:**23689–23697.
Mañes S, Ana Lacalle R, Gomez-Mouton C, and Martinez AC (2003) From rafts to crafts: membrane asymmetry in moving cells. *Trends Immunol* **24:**320–326.
Melkonian KA, Ostermeyer AG, Chen JZ, Roth MG, and Brown DA (1999) Role of lipid modifications in targeting proteins to detergent-resistant membrane rafts. Many raft proteins are acylated, while few are prenylated. *J Biol Chem* **274:**3910–3917.
Milligan G (1996) The stoichiometry of expression of protein components of the stimulatory adenylyl cyclase cascade and the regulation of information transfer. *Cell Signal* **8:**87–95.
Milligan G (2004) Applications of bioluminescence and fluorescence resonance energy transfer to drug discovery at G protein-coupled receptors. *Eur J Pharm Sci* **21:**397–405.
Moffett S, Brown DA, and Linder ME (2000) Lipid-dependent targeting of G proteins into rafts. *J Biol Chem* **275:**2191–2198.
Nebigil CG, Garnovskaya MN, Casanas SJ, Mulheron JG, Parker EM, Gettys TW, and Raymond JR (1995) Agonist-induced desensitization and phosphorylation of human 5-HT1A receptor expressed in Sf9 insect cells. *Biochemistry* **34:**11954–11962.
Newman-Tancredi A, Verriele L, Chaput C, and Millan MJ (1998) Labelling of recombinant human and native rat serotonin 5-HT1A receptors by a novel, selective radioligand, [^{3}H]-S 15535: definition of its binding profile using agonists, antagonists and inverse agonists. *Naunyn Schmiedebergs Arch Pharmacol* **357:**205–217.
Oh P, and Schnitzer JE (2001) Segregation of heterotrimeric G proteins in cell

surface microdomains. G_q binds caveolin to concentrate in caveolae, whereas G_i and G_s target lipid rafts by default. *Mol Biol Cell* **12:**685–698.
Okamoto T, Schlegel A, Scherer PE, and Lisanti MP (1998) Caveolins, a family of scaffolding proteins for organizing "preassembled signaling complexes" at the plasma membrane. *J Biol Chem* **273:**5419–5422.
Ostrom RS, Post SR, and Insel PA (2000) Stoichiometry and compartmentation in G protein-coupled receptor signaling: implications for therapeutic interventions involving G_s. *J Pharmacol Exp Ther* **294:**407–412.
Overstreet DH (2002) Behavioral characteristics of rat lines selected for differential hypothermic responses to cholinergic or serotonergic agonists. *Behav Genet* **32:** 335–348.
Papoucheva E, Dumuis A, Sebben M, Richter DW, and Ponimaskin EG (2004) The 5-hydroxytryptamine$_{1A}$ receptor is stably palmitoylated, and acylation is critical for communication of receptor with Gi protein. *J Biol Chem* **279:**3280–3291.
Pauwels PJ and Colpaert FC (2003) Ca^{2+} responses in Chinese hamster ovary-K1 cells demonstrate an atypical pattern of ligand-induced 5-HT1A receptor activation. *J Pharmacol Exp Ther* **307:**608–614.
Pierce KL, Premont RT, and Lefkowitz RJ (2002) Seven-transmembrane receptors. *Nat Rev Mol Cell Biol* **3:**639–650.
Pucadyil TJ and Chattopadhyay A (2004) Cholesterol modulates ligand binding and G-protein coupling to serotonin$_{1A}$ receptors from bovine hippocampus. *Biochim Biophys Acta* **1663:**188–200.
Pucadyil TJ, Kalipatnapu S, Harikumar KG, Rangaraj N, Karnik SS, and Chattopadhyay A (2004) G-protein-dependent cell surface dynamics of the human serotonin1A receptor tagged to yellow fluorescent protein. *Biochemistry* **43:**15852–15862.
Radley JJ and Jacobs BL (2002) 5-HT1A receptor antagonist administration decreases cell proliferation in the dentate gyrus. *Brain Res* **955:**264–267.
Riad M, Watkins KC, Doucet E, Hamon M, and Descarries L(2001) Agonist-induced internalization of serotonin-1a receptors in the dorsal raphe nucleus (autoreceptors) but not hippocampus (heteroreceptors). *J Neurosci* **21:**8378–8386.
Richter DW, Manzke T, Wilken B, and Ponimaskin E (2003) Serotonin receptors: guardians of stable breathing. *Trends Mol Med* **9:**542–548.
Sambrook J, Fritsch E, and Maniatis T, eds (1989) *Molecular Cloning: A Laboratory Manual.* Cold Spring Harbor Laboratory Press, Cold Spring Harbor, NY.
Shaul PW, Smart EJ, Robinson LJ, German Z, Yuhanna IS, Ying Y, Anderson RG, and Michel T (1996) Acylation targets endothelial nitric-oxide synthase to plasmalemmal caveolae. *J Biol Chem* **271:**6518–6522.
Shenoy-Scaria AM, Dietzen DJ, Kwong J, Link DC, and Lublin DM (1994) Cysteine3 of Src family protein tyrosine kinase determines palmitoylation and localization in caveolae. *J Cell Biol* **126:**353–363.
Sibille E and Hen R (2001) Serotonin$_{1A}$ receptors in mood disorders: a combined genetic and genomic approach. *Behav Pharmacol* **12:**429–438.
Simons K and Toomre D (2000) Lipid rafts and signal transduction. *Nat Rev Mol Cell Biol* **1:**31–39.
Simons K and Vaz WL (2004) Model systems, lipid rafts, and cell membranes. *Annu Rev Biophys Biomol Struct* **33:**269–295.
Song KS, Sargiacomo M, Galbiati F, Parenti M, and Lisanti MP (1997) Targeting of a G alpha subunit (Gi1 alpha) and c-Src tyrosine kinase to caveolae membranes: clarifying the role of N-myristoylation. *Cell Mol Biol* **43:**293–303.
Spiegel S, Kassis S, Wilchek M, and Fishman PH (1984) Direct visualization of redistribution and capping of fluorescent gangliosides on lymphocytes. *J Cell Biol* **99:**1575–1581.
Sprong H, van der Sluijs P, and van Meer G (2001) How proteins move lipids and lipids move proteins. *Nat Rev Mol Cell Biol* **2:**504–513.
van Duyl BY, Rijkers DT, de Kruijff B, and Killian JA (2002) Influence of hydrophobic mismatch and palmitoylation on the association of transmembrane alpha-helical peptides with detergent-resistant membranes. *FEBS Lett* **523:**79–84.
Wedegaertner PB, Bourne HR, and von Zastrow M (1996) Activation-induced subcellular redistribution of Gs alpha. *Mol Biol Cell* **7:**1225–1233.
Yu JZ and Rasenick MM (2002) Real-time visualization of a fluorescent $G\alpha_s$: dissociation of the activated G protein from plasma membrane. *Mol Pharmacol* **61:**352–359.
Zacharias DA, Violin JD, Newton AC, and Tsien RY (2002) Partitioning of lipid-modified monomeric GFPs into membrane microdomains of live cells. *Science* **296:**913–916.

Address correspondence to: Dr. Evgeni Ponimaskin. Abteilung Neuro- und Sinnesphysiologie, Physiologisches Institut, Universität Göttingen, Humboldtallee 23, D-37073 Göttingen, Germany. E-mail: eponima@gwdg.de